Title

Optimization of Secondary Air Injection in a Wood-Burning Cookstove: An Experimental Study.

Journal

Environmental science & technology, 52(7)

ISSN

0013-936X

Authors

Caubel, Julien J
Rapp, Vi H
Chen, Sharon S
et al.

Publication Date

2018-04-01

DOI

10.1021/acs.est.7b05277

Peer reviewed

Optimization of Secondary Air Injection in a Wood-Burning Cookstove: an Experimental Study

Julien J. Caubel†‡, Vi H. Rapp‡, Sharon S. Chen‡, Ashok J. Gadgil‡¶*

† Department of Mechanical Engineering, University of California, Berkeley, Berkeley, California 94720, United States

‡ Environmental Technologies Area, Lawrence Berkeley National Laboratory, Berkeley, California 94720, United States

¶ Department of Civil and Environmental Engineering, University of California, Berkeley, Berkeley, California 94720, United States

*1 Cyclotron Road MS 90R2121, Berkeley, CA 94720

Phone: 01-646-596-3845; E-mail: jcaubel@lbl.gov

ABSTRACT

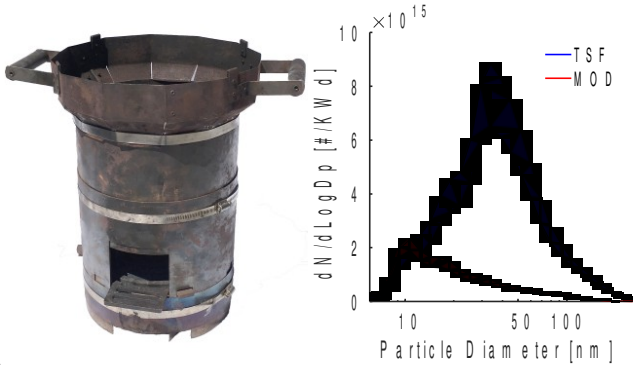

(TOC ART)

Nearly 40% of the world's population regularly cooks on inefficient biomass stoves that emit harmful airborne pollutants, such as particulate matter (PM). Secondary air injection can significantly reduce PM mass emissions to mitigate the health and climate impacts associated with biomass cookstoves. However, secondary air injection can also increase the number of ultrafine particles emitted, which may be more harmful to health. This research investigates the effect of secondary air injection on the mass and size distribution of PM emitted during solid biomass combustion. An experimental biomass cookstove platform and parametric testing approach are presented to identify and optimize critical secondary air injection parameters that reduce PM and other pollutants. Size-resolved measurements of PM emissions were collected and analyzed as a function of parametric stove design settings. The results show that PM emissions are highly sensitive to secondary air injection flow rate and velocity. Although increasing turbulent mixing (through increased velocity) can promote more complete combustion, increasing the total flow rate of secondary air may cause localized flame quenching that increases particle emissions. Therefore, biomass cookstoves that implement secondary air injection should be carefully optimized and validated to ensure that PM emission reductions are achieved throughout the particle size range.

INTRODUCTION

Nearly 40% of the world's population relies on biomass stoves for their daily cooking needs.[1] These stoves are often three stones supporting a cooking pot above a burning bed of solid biomass, known as a three stone fire (TSF). These rudimentary stoves are significant sources of harmful airborne pollutants, such carbon monoxide (CO) and particulate matter (PM).[2] Exposure to indoor air pollution from solid biomass combustion is the world's greatest environmental health risk, causing nearly 4 million premature deaths annually.[3] Many clean and efficient biomass stoves have been designed to reduce exposure to these harmful emissions. Since wood is a common primary cooking fuel, many improved cookstoves are natural draft, wood-burning designs that provide around 50% mass emission reductions relative to a TSF (when normalized by cooking power).[4-6] The World Health Organization (WHO) recommends that 24-hour average PM concentrations remain below 25 $\mu g/m^3$.[7]

However, a TSF can generate average indoor concentrations exceeding 1000 $\mu g/m^3$, and many natural draft, wood-burning cookstoves do not adequately reduce emissions to meet WHO guidelines and significantly alleviate health impacts.[8,9]

Since harmful emissions from biomass stoves are generated by incomplete fuel oxidation, emission reduction strategies generally rely on improvements in the combustion process. Complete fuel oxidation requires an adequate supply of oxygen in the combustion zone, and benefits from: (1) Combustion temperatures above ~850°C, (2) Sufficient residence time for the gas-phase fuel in the combustion zone, and (3) Turbulence to promote mixing of gas-phase fuel and oxygen.[10] In natural draft cookstoves, combustion of the gas-phase fuel is a buoyancy- and diffusion-driven process that generates little turbulence, leading to fuel-rich combustion zones where oxidation is incomplete. Although natural draft cookstoves designed to consume improved

biomass fuels (such as pellets) can reduce harmful emissions, the additional fuel processing cost and lack of distribution infrastructure limit adoption in the poor, remote communities most at risk.[6,11]

In many applications of solid fuel combustion, such as boilers, heaters, and cookstoves, an effective method for reducing unwanted emissions is injecting secondary air into the combustion chamber.[12-17] Carefully positioned, high-velocity jets of secondary air generate turbulent mixing that is typically lacking in naturally drafted, diffusion flames. Air injection also provides oxygen directly to fuel-rich zones, thereby promoting more complete oxidation and higher combustion temperatures.[12,18,19] However, non-preheated secondary air is much cooler than the combustion gases, and when improperly injected, can lead to lower combustion temperatures that result in incomplete fuel oxidation and more pollutant emissions.[20] Furthermore, researchers have shown that secondary air injection can reduce the mass of PM emitted during cooking, but may increase the number of ultrafine particles generated.[21] Inhalation of these ultrafine particles (i.e., with diameters smaller than 100 nm) may lead to long-term respiratory illness.[22] Consequently, it is important to ensure that secondary air injection designs achieve emission reductions throughout the particle size range.

Achieving comprehensive emission reductions using secondary air injection requires many design parameters to be optimized. For example, the airflow rate should be set at an optimal value that promotes effective turbulent mixing, but does not lower combustion zone temperatures excessively. Several publications demonstrate the importance of secondary air injection optimization in combustion appliances that utilize pelletized biomass fuels.[12,13,18,19,23] However, over 2 billion people do not have access to processed fuels, and must instead rely on

unprocessed biomass, such as wood and dung.[24] Despite the potential benefits of air injection, systematic studies of this technology in cookstoves that use unprocessed biomass fuels are not readily available.

In this paper, we present an experimental biomass cookstove platform and parametric testing approach to identify and optimize critical secondary air injection parameters that reduce CO, PM, and black carbon (BC) emissions from unprocessed wood combustion. We conducted over 130 experimental trials, systematically varying several air injection design parameters (e.g., flow rate, velocity, position) to evaluate their effect on cooking performance and emissions. Size-resolved measurements of particle emissions were analyzed as a function of parametric cookstove settings to provide insight on the effects of secondary air injection on particle formation mechanisms, and inform future improved biomass cookstove designs.

MATERIALS AND METHODS

Modular Air Injection Cookstove Design (MOD). The MOD stove, shown in Figure 1, is a continuously fed, wood-burning cookstove designed to enable rapid adjustments of critical air injection design features. The MOD stove's general architecture is based on the Berkeley-Darfur Stove (BDS), using the same firebox design and accommodating the same cast-aluminum Darfuri cooking pot.[6,21] The MOD stove has a cylindrical firebox that is 178 mm (7 inch) in diameter with a front-facing fuel feed, and a cast-iron fuel grate. Above the firebox, there is a conical chimney (see Figure 1(c)) that reduces to a cylindrical extension, or 'throat', 76 mm (3 inch) in diameter. The pot is supported above the throat, and surrounded by a skirt to increase heat transfer efficiency.

Primary air enters the firebox through the open fuel feed and adjustable openings in the stove body located below the fuel grate. Secondary air from a compressed air cylinder flows into

a manifold inside the stove and is injected into the firebox through holes in the conical chimney, as shown in Figure 2. The conical chimney is a removable pipe reducer known as a ‘cone’. These removable cones (one of which is shown in Figure 1(c)) allow for various air injection designs to be implemented and tested rapidly. New air injection patterns are created by drilling holes into a new cone, and mounted inside the manifold.

The MOD stove also incorporates design features to adjust the following parameters: (1) Primary air intake: the size of the opening in the stove body for primary air entrainment can be adjusted using a sliding ring, (2) Grate height: the fuel grate can be moved up and down, adjusting the distance between the fuel bed and the air injection holes in the conical manifold, and (3) Pot height: the pot sits on three bolts to adjust the height of the pot above the throat. Using these design features, shown in Figures S1 to S3, rapid, repeatable, and consistent parametric experiments can be conducted. However, the stove’s complex modular design and reliance on a compressed air cylinder make it uneconomical and impractical for field use. Instead, the lessons learned and design principles extracted from testing of the MOD stove are intended to inform future clean biomass cookstove designs for mass production and distribution.

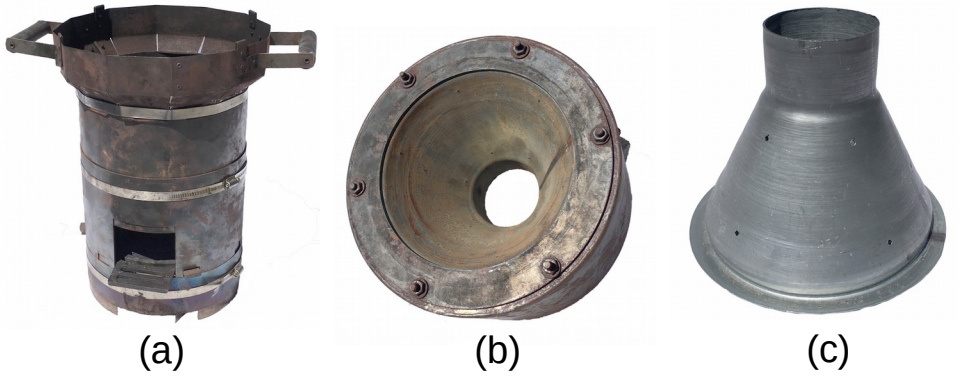

Figure 1. (a) MOD stove (b) Air injection manifold (c) Air injection cone

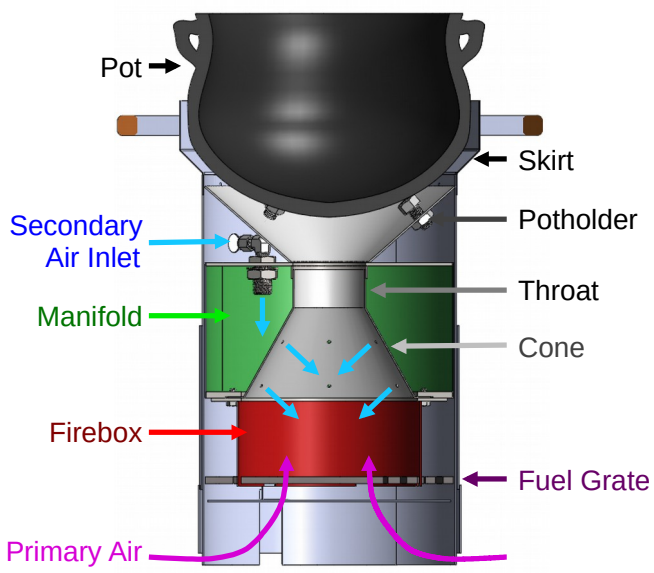

Figure 2. Cut view of MOD stove

Experimental Set Up. All experiments were conducted at the cookstove testing facility at Lawrence Berkeley National Laboratory (LBNL), schematically represented in Figure S4. Cookstoves are tested under a steel exhaust hood that completely captures pollutant emissions. Electric blowers exhaust emissions outside the building using a steel duct system. The flow rate through the duct is calculated using differential pressure measurements across a calibrated iris damper, and set to 5660 LPM (200 CFM) throughout testing to ensure replicability of measurements.

Particulate and gaseous emission concentrations in the duct are measured every second (1 Hz) using a suite of real-time instruments. Carbon monoxide (CO) and carbon dioxide (CO_2) volume concentrations are measured using a California Analytical Instruments 600 Series gas analyzer. Real-time PM instruments sample emissions from the duct isokinetically using a secondary diluter (see Appendix III of the SI). Particle number concentrations are measured as a function of particle diameter from 5 nm to 2.5 µm using a TSI 3091 Fast Mobility Particle Sizer (FMPS), and a TSI 3321 Aerodynamic Particle Sizer (APS). BC mass concentrations are

measured using a Magee Scientific AE-22 Aethalometer. The total mass of PM with aerodynamic diameter ≤ 2.5 μm ($PM_{2.5}$) emitted during each cookstove experiment is measured gravimetrically using 47-mm filters. The gravimetric filter system samples PM emissions from the duct isokinetically using a dedicated probe. Detailed overviews of the experimental set-up and gravimetric $PM_{2.5}$ measurement procedures are provided in section S-1.2 of the SI.

Stove Testing Procedure. Cookstove performance and emissions were measured during the high power, cold start phase of the Water Boiling Test (WBT) 4.2.3.[25]

During this test phase, a fire is lit inside a stove that is initially at ambient temperature ('cold'), and operated at a high firepower to boil 5 L of water. The test ends when a full rolling boil is reached at a measured water temperature of 99°C (the nominal local boiling point). Pollutant emissions are typically more elevated during this phase of stove use because: (1) the cold stove and pot of water quench flames and absorb heat, thereby lowering combustion temperatures, (2) the cold fuel bed combusts poorly during initial lighting, and (3) the mass of harmful emissions released per energy delivered to the pot of water typically increases with firepower.[6] In this way, the cold start phase represents a 'worst-case' emissions scenario, and the design principles derived can be applied to other phases of stove use that are more forgiving to performance (e.g., hot start or simmer).

For each experiment, the stove was fueled with Douglas Fir wood cut into uniform pieces and dried to 7-9% moisture content on a wet basis. All tests were conducted at a constant high firepower setting of 5 kW to enable the immediate comparison of stove configurations.[21] A compressed air cylinder provided secondary air for the MOD stove using a two-stage regulator. The volumetric flow rate of secondary air was measured using a rotameter and adjusted using a valve. During preliminary trials, we observed that turning on the secondary air injection too soon

after ignition caused the fire to smolder or go out entirely. Consequently, air injection was initiated about 2 minutes after fuel ignition to ensure the fire was well established, thereby preventing quenching and extinction.

Parametric Testing Procedure. Five MOD stove design parameters were identified for experimental optimization: (1) Pot height, (2) Grate height, (3) Primary air intake size, (4) Secondary air injection pattern (number and arrangement of holes), and (5) Secondary air flow rate. Since testing results from solid biomass stoves are highly variable, replicate tests are required to accurately determine performance and emission levels at any given parametric stove configuration. In order to reduce the total testing time required to optimize the stove, exploratory trials were conducted using a simplified cold start procedure (see SI section S-1.4).

During exploratory testing, stove design parameters were methodically adjusted to reduce pollutant emissions while maintaining high thermal efficiency. Using data from 71 exploratory trials, optimal settings were identified for the following air injection design parameters: The gap between the pot and skirt is set to 15 mm (0.60 inch), the grate height is set to 57 mm (2.25 inch) below the air injection manifold, and the primary air intake is set to roughly 70% of the fully open position (an opening with an area of 4800 mm^2 (7.4 $inch^2$)). Furthermore, two clean and efficient air injection patterns were identified for further parametric testing (shown in Figure S6). All exploratory testing results are provided in the SI.

Following exploratory testing, the two optimal air injection patterns were tested at flow rates of 21, 28, and 35 LPM (0.75, 1, and 1.25 CFM), for a total of six parametric configurations; all other parameters were maintained at the optimal values identified during exploratory testing. For each parametric configuration, 6 to 7 replicate tests were conducted. By adjusting the stove parameters in evenly distributed increments, parametric curves were generated to illuminate how

secondary air injection influences the stove's emissions and performance. Results from these initial 39 trials suggest that an air injection flow rate of 28 LPM is most effective, and so an additional 12 trials were conducted at this flow rate using both air injection patterns. These two final sets of 12 replicate tests enable the identification and validation of the optimal parametric stove configuration with a higher degree of confidence.

Data Analysis and Metrics. All stove performance and emissions metrics were calculated in accordance with the methods presented in section S-1.6 of the SI. Emission factors are normalized by the average thermal power delivered to the pot, known as cooking power, in units of kW-delivered (kWd). Cooking power is defined as the product of firepower and thermal efficiency, and represents the useful thermal power output of the cookstove. All data are presented with 90% confidence intervals calculated using Student's t-distribution.[26,27]

The MOD stove's performance and emissions are compared to those of a TSF using cold start testing data collected by Rapp et al. (2016) at the LBNL cookstove facility. The TSF was also tested at a firepower of 5 kW, with the same pot, fuel, experimental procedures, and instruments as used for the MOD stove testing.[21]

RESULTS AND DISCUSSION

Parametric Performance Metrics. A total of 63 WBT cold start tests were conducted to identify the cleanest, most efficient combination of secondary air injection pattern and flow rate. The thermal efficiency and emissions of six MOD stove configurations are evaluated as a function of air injection flow rate and velocity, as shown in Figure 3. The air injection velocity is calculated using the air injection flow rate and total area of the holes in the air injection pattern, as outlined in section S-1.6 of the SI. Emission factors represent the total mass of pollutant emitted during the cold start test, normalized by the cooking power.

Firepower, shown in Figure 3(a), was maintained at 5.1±0.1 kW throughout parametric testing to provide consistency between experiments. Figure 3(b) shows that thermal efficiency remains around 27% for flow rates of 21 and 28 LPM, and decreases to about 24% at 35 LPM. The decrease in thermal efficiency at 35 LPM is likely caused by the abundance of injected air cooling the combustion zone, thereby reducing the stove's exhaust temperature even as firepower is held constant. The drop in exhaust temperature reduces the rate of heat transfer to the pot, and degrades the thermal performance of the stove.

Increasing CO emissions, shown in Figure 3(c), also suggest that air injection at 35 LPM is quenching the flame and cooling the combustion zone.[18,28] CO emissions from biomass combustion increase dramatically when combustion temperatures drop below ~800°C, but remain relatively constant above this critical oxidation temperature.[15,20] Correspondingly, Figure 3(c) shows that CO emissions are relatively constant as air injection increases from 21 to 28 LPM, but more than double when flow rate increases from 28 to 35 LPM. Additionally, as air injection velocity increases from 20 to 25 m/s at 35 LPM, the magnitude and variability of CO emissions both increase substantially, suggesting that enhanced turbulent mixing of excess secondary air is quenching the flame.

$PM_{2.5}$ emissions follow the same trend as CO emissions: When the flow rate is increased from 28 to 35 LPM at a constant velocity of 20 m/s, $PM_{2.5}$ emissions nearly double, and continue to rise as air injection velocity increases at 35 LPM (see Figure 3(d)). PM formation and growth occur when volatile gases in the exhaust cool and nucleate into solid particles or condense onto existing particles.[29] Similarly to CO, many volatile organic compounds that form PM, such as polycyclic aromatic hydrocarbons (PAH), oxidize around 750-800°C. At a flow rate of 35 LPM, excessive secondary air injection likely lowers the combustion zone temperature below this

224critical oxidation point, thereby enhancing particle nucleation and condensation.[20] Earlier studies
225have also shown that high CO emissions are usually accompanied by higher emissions of volatile
226organic compounds and other carbonaceous species that contribute to $PM_{2.5}$ mass emissions.[20,28]

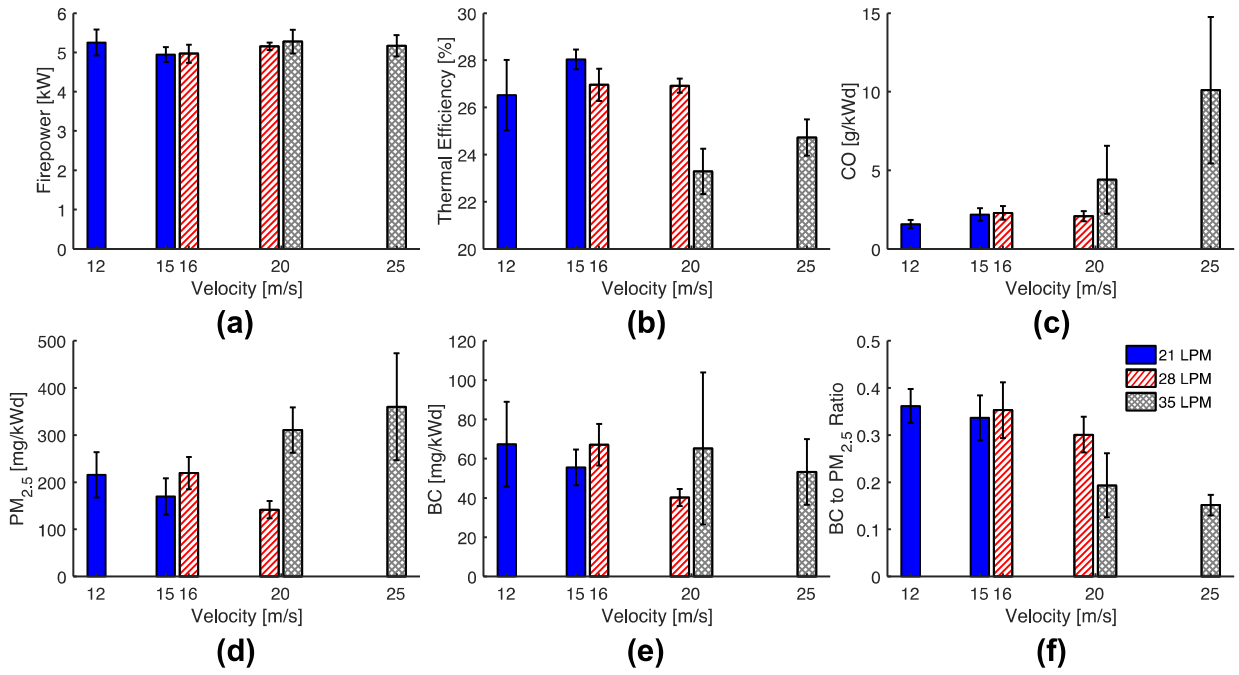

227

228**Figure 3.** Cold start performance and emissions of the MOD stove as a function of secondary air
229injection flow rate (represented by bar color) and velocity (shown on the horizontal axis): (a)
230Firepower (kW); (b) Thermal efficiency (%), (c) Carbon monoxide (CO) emissions (g/kWd), (d)
231Particulate matter ($PM_{2.5}$) emissions (mg/kWd), (e) Black carbon (BC) emissions (mg/kWd), (f)
232BC to $PM_{2.5}$ ratio. Bar heights represent the metric mean at each stove configuration, and error
233bars represent the corresponding 90% confidence interval. Emissions are reported as the total
234mass of pollutant emitted during the cold start test normalized by the cooking power.

235 $PM_{2.5}$ composition can also provide insight into combustion conditions. $PM_{2.5}$ emissions
236from biomass combustion contain both inorganic particles, such as salt compounds and heavy
237metals, and organic particles consisting of either BC or tars.[30] The effect of air injection flow rate

and velocity on BC emissions – optically absorbing soot that forms directly in the flame – is shown in Figure 3(e). At each flow rate setting, BC emissions decrease with increasing air injection velocity, as additional oxygen and turbulent mixing help to eliminate fuel-rich zones where BC is formed.[31] However, BC emissions at the low velocity setting for each air injection flow rate remain nearly constant (~70 mg/kWd). As flow rate increases, combustion zone temperatures are lowered, and the rate of BC oxidation decreases.[32,33] For these combustion conditions, the resulting increase in BC emissions effectively negates the reductions incurred from increasing turbulent mixing.[15,34]

Unlike CO and $PM_{2.5}$, BC emissions at a secondary air flow rate of 35 LPM generally decrease when injection velocity increases from 20 to 25 m/s, suggesting that combustion zone temperatures are sufficiently elevated to oxidize BC. BC from biomass combustion has been shown to oxidize around 350 °C.[34,35] This oxidation temperature is much lower than that of CO and many of the volatile compounds that form $PM_{2.5}$ (around 750 - 800 °C), and enables BC reductions throughout the parametric range.

In order to better understand the effect of secondary air injection on $PM_{2.5}$ composition, the ratio of BC to $PM_{2.5}$ emissions is shown in Figure 3(f). The figure shows that the BC to $PM_{2.5}$ ratio is stable at air injection flow rates of 21 and 28 LPM, but decreases sharply at 35 LPM. This trend further illustrates that BC is effectively oxidized throughout the parametric range, but excessive cooling at a flow rate of 35 LPM quenches the flame and increases overall $PM_{2.5}$ mass emissions. Furthermore, the BC to $PM_{2.5}$ ratio at each flow rate setting remains relatively constant as air injection velocity increases, suggesting that $PM_{2.5}$ composition is more dependent on combustion temperature than turbulent mixing.

Overall, the metrics in Figure 3 indicate that a flow rate of 28 LPM at an air injection velocity of 20 m/s is the optimal configuration for this stove. In this configuration, the stove minimizes emissions of pollutants, while maintaining high thermal efficiency. Although thermal efficiency and CO emissions improve slightly at a flow rate 21 LPM, the metrics show that 28 LPM at 20 m/s provides an optimal balance between maintaining high thermal performance and lowering pollutant emissions. Compared to a TSF, the optimal configuration of the MOD stove uniformly reduces CO, $PM_{2.5}$, and BC emissions by about 90%, while increasing thermal efficiency from 23.3 ± 0.7% to 26.4 ± 0.4% (see section S-2.3 of the SI).

Size-Resolved Particle Emissions with Varying Air Injection Flow Rate. The optimal injection pattern identified in Figure 3 (Cone 1, shown in Figure S6) was tested at 21, 28, and 35 LPM (corresponding to air injection velocities of 15, 20, and 25 m/s, respectively). Figure 4 shows the mean particle distribution of replicate trials conducted at each air injection flow rate, with shaded areas representing 90% confidence intervals of the set. Each distribution represents the total particle number and volume emitted over the cold start, normalized by the cooking power. FMPS measurements span from 6 to 295 nm, while APS measurements span from 351 to 2500 nm. The last four bins of the FMPS measurement span (from 341 to 524 nm) are omitted, and the APS measurements have been converted from aerodynamic to electrical mobility particle diameter (see section S-1.7 of the SI).[36]

Figure 4(a) reveals that the number distribution at each secondary air injection flow rate setting has a maximum peak at a particle diameter of around 10 nm, representing primary particles formed by the nucleation of volatile gases in the exhaust or soot generation in the flame.[37-39] Furthermore, the figure illustrates that as flow rate increases, the number of particles from 10 to 50 nm also increases. These results suggest that combustion zone temperatures

283decrease with increasing flow rate, thereby inhibiting the oxidation of volatile organic gases and
284other PM-forming species.[15] The increased emission of volatile gases and lower combustion zone
285temperatures both promote more PM nucleation.[20,28] The number distribution at flow rate of 35
286LPM has two prominent peaks at particle diameters of around 20 and 30 nm that diminish as
287flow rate decreases. These two peaks likely represent primary particle species that begin to form
288as combustion zone temperatures decrease at higher air injection flow rates.[31,39]

289 The particle volume distributions in Figure 4(b) show a unimodal peak centered at a
290particle diameter of around 100 nm, closely mirroring particle distribution measurements from
291other biomass combustion studies.[15,28,38,40] The figure also shows that a secondary air injection
292flow rate of 28 LPM yields the lowest volume distribution, indicating that this provides sufficient
293turbulent mixing to promote better fuel oxidation without lowering combustion zone
294temperatures excessively. The increased particle volume generation at both 21 LPM and 35 LPM
295suggests that 21 LPM does not provide enough turbulent mixing while 35 LPM cools the
296combustion zone.

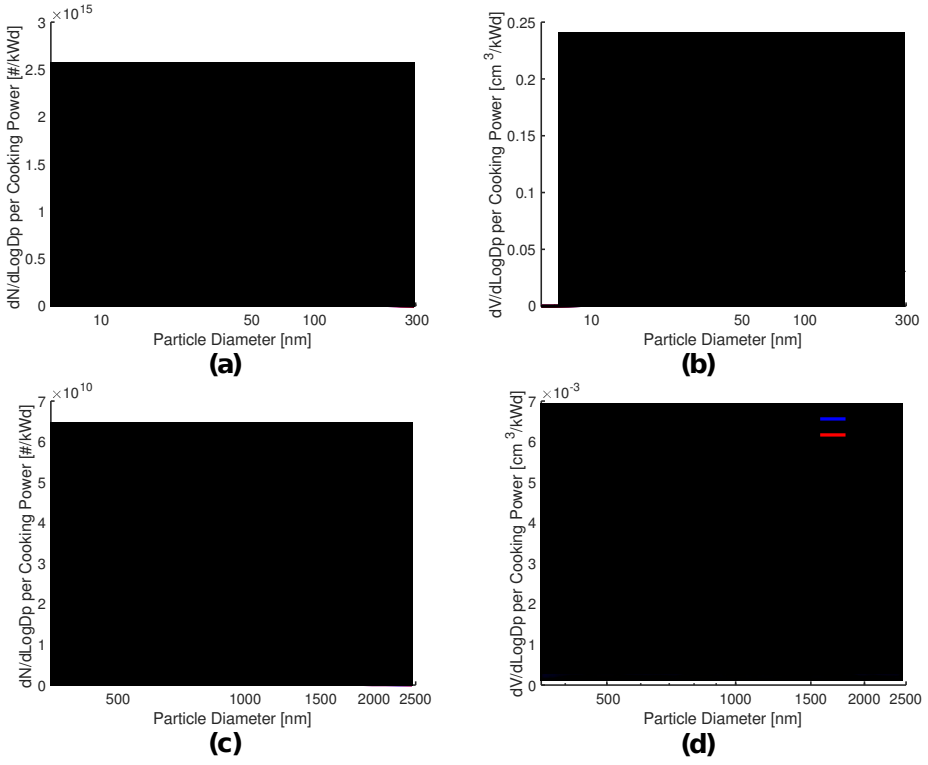

297

298 **Figure 4.** Size-resolved distribution of total particle number or volume emitted during the cold
299 start, normalized by the average cooking power, for three air injection flow rate settings: (a)
300 FMPS particle number distribution, (b) FMPS particle volume distribution, (c) APS particle
301 number distribution, (d) APS particle volume distribution

302 Figure 4(c) and 4(d) show that the number and volume distributions of particles larger
303 than 350 nm (up to 2500 nm) are roughly similar for flow rates of 21 and 28 LPM, but increase
304 appreciably at 35 LPM, further indicating that combustion zone temperatures drop below the
305 critical oxidation temperature of certain PM forming species.[28] The distinct peak in the volume
306 distribution at 1280 nm (see Figure 4(d)) is the result of primary particle growth through
307 condensation and agglomeration, promoted by the low combustion temperatures and high
308 turbulent mixing at a flow rate of 35 LPM.[38,39]

Size-Resolved Particle Emissions with Varying Air Injection Velocity. Air injection flow rate was maintained at the optimal 28 LPM setting, while velocity was varied using the two different air injection patterns. Figure 5 provides the resulting particle number and volume distributions at secondary air injection velocities of 16 and 20 m/s. For both air injection velocities, the peaks in the particle number distributions at a diameter of 10 nm are nearly identical (see Figure 5(a)). However, increasing air injection velocity reduces particle number emissions above 30 nm. Additionally, the peaks at particle diameters of 20 nm and 30 nm become less distinguishable as air injection velocity increases from 16 m/s to 20 m/s. These results indicate that additional turbulent mixing at higher air injection velocity promotes more oxidation of volatile gases, and reduces the formation of primary particles and subsequent particle growth through condensation.[15,28] Correspondingly, Figure 5(b) shows that increasing air injection velocity reduces the particle volume distribution by almost 50%.

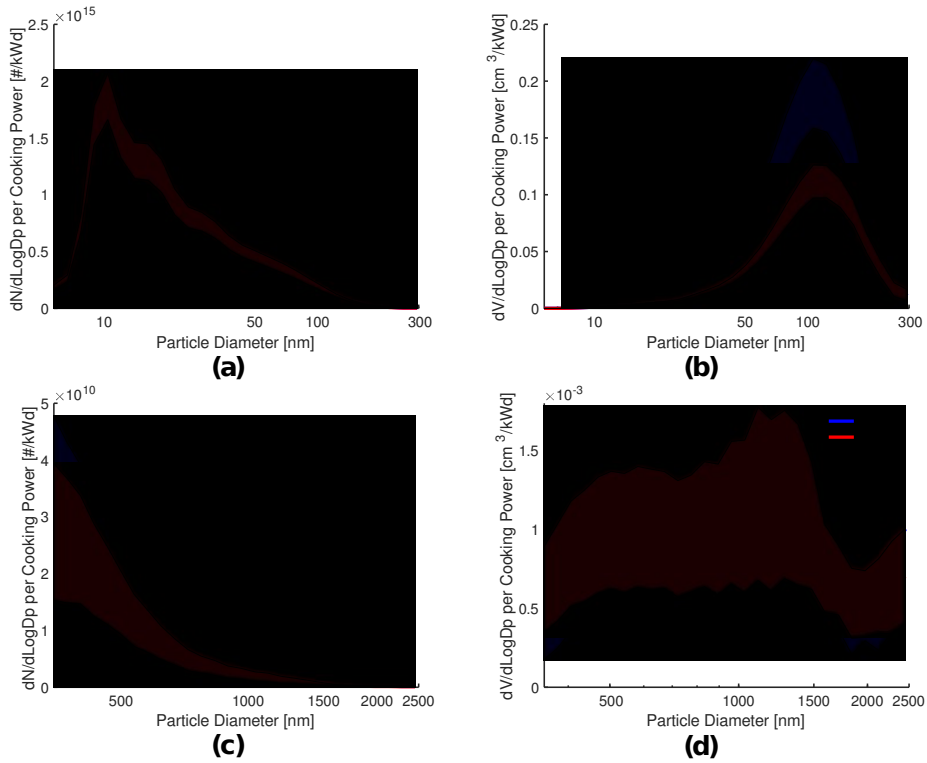

Figure 5. Size-resolved distribution of total particle number or volume emitted during the cold start, normalized by the average cooking power, for two air injection velocity settings at a flow rate of 28 LPM: (a) FMPS particle number distribution, (b) FMPS particle volume distribution, (c) APS particle number distribution, (d) APS particle volume distribution

For particles larger than 350 nm (up to 2500 nm), the particle number and volume distributions at both air injection velocities are nearly identical (see Figure 5(c) and 5(d)). These results indicate that air injection at 28 LPM promotes more complete fuel oxidation and reduces particle growth above 350 nm, independently of air injection velocity. However, for a flow rate of 21 LPM, the number of particles larger than 350 nm increases significantly as air injection velocity decreases, suggesting that a lack of turbulent mixing can promote particle growth under certain conditions (see Figure S9). Particle number and volume distributions for the air injection velocities tested at 21 LPM and 35 LPM are provided in section S-2.4 of the SI.

Size-Resolved Particle Emissions compared to Three-Stone Fire. Figure 4 and 5 show that the MOD stove provides the greatest particle emission reductions at a secondary air injection flow rate of 28 LPM and injection velocity of 20 m/s (which agrees with the gravimetric $PM_{2.5}$ measurements provided in Figure 3(d)). However, it should also be noted that the emission of particles smaller than 50 nm in diameter are somewhat lower for an air injection flow rate of 21 LPM, highlighting the importance of maintaining high combustion zone temperatures to minimize ultrafine particle emissions.

Figure 6 compares FMPS particle number and volume distributions of the optimal MOD stove configuration (28 LPM and 20 m/s) to the TSF. Figure 6(a) shows that the MOD stove reduces the total number of ultrafine particles (with a diameter less than 100 nm) by about 75% relative to the TSF. However, for particles less than 10 nm in diameter, the MOD stove generates

roughly the same number of particles as the TSF. Given the MOD stove's improved combustion conditions (as demonstrated by the significant emissions reductions), it is possible that these 10 nm particles nucleate from inorganic volatile gases, such as salts. These inorganic compounds volatilize more readily at higher fuel bed temperatures, and result in particle emissions that cannot be reduced through improvements in the combustion process.[12,14,30,40]

Figure 6(b) shows that volumetric particle emissions are reduced by an order of magnitude throughout the diameter range provided, which agrees with the gravimetric particle measurements provided in Table S2. For particles larger than 350 nm in diameter, the MOD stove uniformly reduces particle number and volume generation by nearly two orders of magnitude. Number and volume distributions for particles larger than 350 nm can be found in section S-2.5 of the SI.

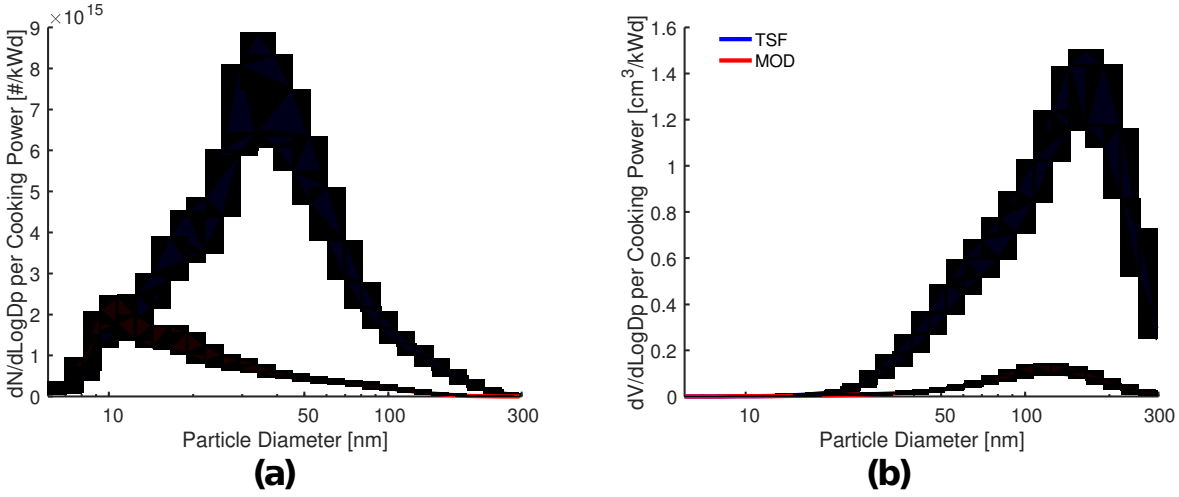

Figure 6. Size-resolved distribution of total particle number or volume emitted during the cold start, normalized by the average cooking power for a three-stone fire (TSF) and the MOD stove operating at an air injection flow rate of 28 LPM and velocity of 20 m/s: (a) FMPS particle number distribution, (b) FMPS particle volume distribution

Using the experimentally optimized configuration, the MOD stove reduces CO, $PM_{2.5}$, and BC mass emissions by about 90%, and reduces ultrafine particle number emissions by about 75%, compared to a TSF. The results also demonstrate that pollutant emissions are highly sensitive to secondary air injection design parameters, such as flow rate and velocity. Therefore, improved cookstove designs that implement air injection should be experimentally optimized and validated to ensure that pollutant mass emissions are minimized, and particle emissions are reduced across the full range of PM diameters. While this study focuses on modulating five stove design parameters to reduce emissions, it is also important to investigate other operational factors, such as firepower, fuel condition (moisture content, size, surface area), and secondary air temperature. Furthermore, future studies should incorporate additional instrumentation to enable deeper investigation of the combustion process, such as thermocouples to measure combustion temperatures, and/or a thermal-optical analyzer to examine the composition of PM emitted.

Overall, this study demonstrates that experimental optimization enables the design of wood-burning stoves that both reduce pollutant emissions and improve cooking performance. The experimental approach and results presented can inform the development of air injection stoves that reduce harmful smoke exposure in the one billion households currently relying on biomass cooking fuels.

SUPPORTING INFORMATION

Additional information on the Modular stove design, experimental setup, and results are available in the Supporting Information. This material is available free of charge via the Internet at http://pubs.acs.org/.

ACKNOWLEDGMENT

This work was performed at the Lawrence Berkeley National Laboratory, operated by the University of California, under DOE Contract DE-AC02-05CH11231. We gratefully acknowledge support for this work from DOE's Biomass Energy Technologies Office. Author Julien J. Caubel is grateful for support from the National Science Foundation’s Graduate Research Fellowship Program.

The authors acknowledge Brahim Idrissi Kaitouni, Allen Boltz, and Arjun Kaul for their countless hours in the laboratory testing the cookstoves and collecting data. We would also like to thank Dr. Thomas Kirchstetter for guidance in post-processing the particle emissions data and Gary Hubbard for developing the software tools to simplify data collection from all of our instruments.

ABBREVIATIONS

APS, Aerodynamic Particle Sizer; BC, Black Carbon; BDS, Berkeley-Darfur Stove; CAI, California Analytical Instruments; CO_2, Carbon Dioxide; CO, Carbon Monoxide; EC, Elemental Carbon; FMPS, Fast Mobility Particle Sizer; kWd, kilowatt of power delivered to the pot; LBNL, Lawrence Berkeley National Laboratory; MOD, Modular Stove; PAH, Polycyclic Aromatic Hydrocarbon; PM, Particulate Matter; $PM_{2.5}$, Particulate Matter with an aerodynamic diameter ≤ 2.5 μm; ppm, parts per million; TSF, Three Stone Fire; WBT, Water Boiling Test.

400**REFERENCES**

401(1) Bonjour, S.; Adair-Rohani, H.; Wolf, J.; Bruce, N. G.; Mehta, S.; Prüss-Ustün, A.;
402 Lahiff, M.; Rehfuess, E. A.; Mishra, V.; Smith, K. R. Solid Fuel Use for Household
403 Cooking: Country and Regional Estimates for 1980–2010. *Environ. Health Perspect.*
404 **2013**, *121* (7), 784–790.
405(2) Bruce, N. G.; Perez-Padilla, R.; Albalak, R. Indoor air pollution in developing countries:
406 a major environmental and public health challenge. *Bulletin of the World Health*
407 *Organization* **2000**, *78* (9), 1078–1092.
408(3) Lim, S. S.; Vos, T.; Flaxman, A. D.; Danaei, G.; Shibuya, K.; Adair-Rohani, H.;
409 AlMazroa, M. A.; Amann, M.; Anderson, R. H.; Andrews, K. G.; et al. A comparative
410 risk assessment of burden of disease and injury attributable to 67 risk factors and risk
411 factor clusters in 21 regions, 1990–2010: a systematic analysis for the Global Burden of
412 Disease Study 2010. *The Lancet* **2012**, *380* (9859), 2224–2260.
413(4) Legros, G.; Havet, I.; Bruce, N. G.; Bonjour, S. *The Energy Access Situation in*
414 *Developing Countries*; United Nations Development Programme (UNDP): New York,
415 2009; pp 1–142.
416(5) Birol, F.; Argiri, M.; Cozzi, L.; Dowling, P.; Emoto, H.; Lyons, L.; Malyshev, T. *World*
417 *Energy Outlook 2006*; Priddle, R., Ed.; International Energy Agency, 2006; pp 1–601.
418(6) Jetter, J.; Zhao, Y.; Smith, K. R.; Khan, B.; Yelverton, T.; DeCarlo, P.; Hays, M. D.
419 Pollutant Emissions and Energy Efficiency under Controlled Conditions for Household
420 Biomass Cookstoves and Implications for Metrics Useful in Setting International Test
421 Standards. *Environ. Sci. Technol.* **2012**, *46* (19), 10827–10834.
422(7) *WHO Air quality guidelines for particulate matter, ozone, nitrogen dioxide and sulfur*
423 *dioxide*; World Health Organization, 2005.

(8) Smith, K. R.; Dutta, K.; Chengappa, C.; Gusain, P. P. S.; Berrueta, O. M. A. V.; Edwards, R.; Bailis, R.; Shields, K. N. Monitoring and evaluation of improved biomass cookstove programs for indoor air quality and stove performance: conclusions from the Household Energy and Health Project. *Energy for Sustainable Development* **2007**, *11* (2), 5–18.

(9) Chen, C.; Zeger, S.; Breysse, P.; Katz, J.; Checkley, W.; Curriero, F. C.; Tielsch, J. M. Estimating Indoor PM2.5 and CO Concentrations in Households in Southern Nepal: The Nepal Cookstove Intervention Trials. *PLoS ONE* **2016**, *11* (7), e0157984–17.

(10) Nussbaumer, T. Combustion and Co-combustion of Biomass: Fundamentals, Technologies, and Primary Measures for Emission Reduction †. *Energy Fuels* **2003**, *17* (6), 1510–1521.

(11) Edwards, R.; Karnani, S.; Fisher, E. M.; Johnson, M.; Naeher, L.; Smith, K. R.; Morawska, L. *WHO Indoor Air Quality Guidelines: Household fuel Combustion*; World Health Organization, 2014; pp 1–42.

(12) Lamberg, H.; Sippula, O.; Tissari, J.; Jokiniemi, J. Effects of Air Staging and Load on Fine-Particle and Gaseous Emissions from a Small-Scale Pellet Boiler. *Energy Fuels* **2011**, *25* (11), 4952–4960.

(13) Lyngfelt, A.; Leckner, B. Combustion of wood-chips in circulating fluidized bed boilers — NO and CO emissions as functions of temperature and air-staging. *Fuel* **1999**, No. 78, 1065–1072.

(14) Carroll, J. P.; Finnan, J. M.; Biedermann, F.; Brunner, T.; Obernberger, I. Air staging to reduce emissions from energy crop combustion in small scale applications. *Fuel* **2015**, *155*, 37–43.

(15) Nuutinen, K.; Jokiniemi, J.; Sippula, O.; Lamberg, H.; Sutinen, J.; Horttanainen, P.;

447 Tissari, J. Effect of air staging on fine particle, dust and gaseous emissions from
448 masonry heaters. *Biomass and Bioenergy* **2014**, *67*, 167–178.
449(16) Sutar, K. B.; Kohli, S.; Ravi, M. R.; Ray, A. Biomass cookstoves: A review of technical
450 aspects. *Renewable and Sustainable Energy Reviews* **2015**, *41*, 1128–1166.
451(17) Still, D.; Bentson, S.; Li, H. Results of Laboratory Testing of 15 Cookstove Designs in
452 Accordance with the ISO/IWA Tiers of Performance. *EcoHealth* **2015**, *12*, 12–24.
453(18) Okasha, F. Staged combustion of rice straw in a fluidized bed. *Experimental Thermal*
454 *and Fluid Science* **2007**, *32* (1), 52–59.
455(19) Tryner, J.; Tillotson, J. W.; Baumgardner, M. E.; Mohr, J. T.; DeFoort, M. W.; Marchese,
456 A. J. The Effects of Air Flow Rates, Secondary Air Inlet Geometry, Fuel Type, and
457 Operating Mode on the Performance of Gasifier Cookstoves. *Environ. Sci. Technol.*
458 **2016**, *50* (17), 9754–9763.
459(20) Pettersson, E.; Lindmark, F.; Öhman, M.; Nordin, A.; Westerholm, R.; Boman, C.
460 Design Changes in a Fixed-Bed Pellet Combustion Device: Effects of Temperature and
461 Residence Time on Emission Performance. *Energy Fuels* **2010**, *24* (2), 1333–1340.
462(21) Rapp, V. H.; Caubel, J. J.; Wilson, D. L.; Gadgil, A. J. Reducing Ultrafine Particle
463 Emissions Using Air Injection in Wood-Burning Cookstoves. *Environ. Sci. Technol.*
464 **2016**, *50* (15), 8368–8374.
465(22) Valavanidis, A.; Fiotakis, K.; Vlachogianni, T. Airborne Particulate Matter and Human
466 Health: Toxicological Assessment and Importance of Size and Composition of Particles
467 for Oxidative Damage and Carcinogenic Mechanisms. *Journal of Environmental*
468 *Science and Health, Part C* **2008**, *26* (4), 339–362.
469(23) Wiinikka, H.; Gebart, R. Critical Parameters for Particle Emissions in Small-Scale

Fixed-Bed Combustion of Wood Pellets. *Energy Fuels* **2004**, *18* (4), 897–907.

(24) Malla, S.; Timilsina, G. R. *Household Cooking Fuel Choice and Adoption of Improved Cookstoves in Developing Countries*; The World Bank, 2014; pp 1–52.

(25) *The Water Boiling Test*, 4 ed.; Global Alliance for Clean Cookstoves, 2014; pp 1–89.

(26) Taylor, J. R. *An introduction to error analysis: The study of uncertainties in physical measurements*; University Science Books: Sausalito, CA, 1997; pp 1–1.

(27) Wang, Y.; Sohn, M. D.; Wang, Y.; Lask, K. M.; Kirchstetter, T. W.; Gadgil, A. J. How many replicate tests are needed to test cookstove performance and emissions? — Three is not always adequate. *Energy for Sustainable Development* **2014**, *20*, 21–29.

(28) Johansson, L. S.; Leckner, B.; Gustavsson, L.; Cooper, D.; Tullin, C.; Potter, A. Emission characteristics of modern and old-type residential boilers fired with wood logs and wood pellets. *Atmospheric Environment* **2004**, *38* (25), 4183–4195.

(29) Torvela, T.; Tissari, J.; Sippula, O.; Kaivosoja, T.; Leskinen, J.; Virén, A.; Lähde, A.; Jokiniemi, J. Effect of wood combustion conditions on the morphology of freshly emitted fine particles. *Atmospheric Environment* **2014**, *87*, 65–76.

(30) Kelz, J.; Brunner, T.; Obernberger, I.; Jalava, P.; Hirvonen, M. R. PM emissions from old and modern biomass combustion systems and their health effects. **2010**.

(31) Obaidullah, M.; Bram, S.; Verma, V. K.; De Ruyck, J. A Review on Particle Emissions from Small Scale Biomass Combustion. *International Journal of Renewable Energy Research* **2012**, *2* (1), 1–13.

(32) Jiang, M.; Wu, Y.; Lin, G.; Xu, L.; Chen, Z.; Fu, F. Pyrolysis and thermal-oxidation characterization of organic carbon and black carbon aerosols. *Science of the Total Environment, The* **2011**, *409* (20), 4449–4455.

493(33) Brunner, T.; Barnthaler, G.; Obernberger, I. Evaluation of Parameters Determining PM
494 Emissions and their Chemical Composition in Modern Residential Biomass Heating
495 Appliances; 2008; pp 81–86.
496(34) Petzold, A.; Ogren, J. A.; Fiebig, M.; Laj, P.; Li, S. M.; Baltensperger, U.; Holzer-Popp,
497 T.; Kinne, S.; Pappalardo, G.; Sugimoto, N.; et al. Recommendations for reporting
498 “black carbon” measurements. *Atmos. Chem. Phys.* **2013**, *13* (16), 8365–8379.
499(35) Elmquist, M.; Cornelissen, G.; Kukulska, Z.; Gustafsson, Ö. Distinct oxidative stabilities
500 of char versus soot black carbon: Implications for quantification and environmental
501 recalcitrance. *Global Biogeochem. Cycles* **2006**, *20* (2), 1–11.
502(36) Khlystov, A.; Stanier, C.; Pandis, S. N. An Algorithm for Combining Electrical Mobility
503 and Aerodynamic Size Distributions Data when Measuring Ambient Aerosol. *Aerosol*
504 *Science and Technology* **2004**, *38* (S1), 229–238.
505(37) Just, B.; Rogak, S.; Kandlikar, M. Characterization of Ultrafine Particulate Matter from
506 Traditional and Improved Biomass Cookstoves. *Environ. Sci. Technol.* **2013**, *47*, 3506–
507 3512.
508(38) Jöller, M.; Brunner, T.; Obernberger, I. Modeling of aerosol formation during biomass
509 combustion for various furnace and boiler types. *Fuel Processing Technology* **2007**, *88*,
510 1136–1147.
511(39) Obernberger, I.; Brunner, T.; Barnthaler, G. Fine Particulate Emissions From Modern
512 Austrian Small-Scale Biomass Combustion Plants; 2011; Vol. 15, pp 1–12.
513(40) Wiinikka, H.; Gebart, R. The Influence of Air Distribution Rate on Particle Emissions in
514 Fixed Bed Combustion of Biomass. *Combustion Science and Technology* **2005**, *177* (9),
515 1747–1766.

53

516

54